Synthesis and characterization of new imidazolium based protic ionic liquids obtained by nitro- and cyano-functionalization

Citation for the original published paper (version of record):
Dahlqvist, E., Maurina Morais, E., Martinelli, A. (2024). Synthesis and characterization of new imidazolium based protic ionic liquids obtained by nitro- and cyano-functionalization. Journal of Molecular Liquids, 415.
http://dx.doi.org/10.1016/j.molliq.2024.126269

Journal of Molecular Liquids 415 (2024) 126269

Contents lists available at ScienceDirect

Journal of Molecular Liquids

journal homepage: www.elsevier.com/locate/molliq

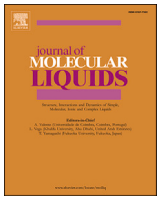

Synthesis and characterization of new imidazolium based protic ionic liquids obtained by nitro- and cyano-functionalization

Eva Dahlqvist [1], Eduardo Maurina Morais [1], Anna Martinelli *

Department of Chemistry and Chemical Engineering, Chalmers University of Technology, 412 96 Gothenburg, Sweden

ARTICLE INFO

Keywords:
Protic ionic liquids
Acidity
Conductivity
Synthesis

ABSTRACT

The prevailing strategies for synthesizing Brønsted acidic ionic liquids have primarily relied on SO_3H functionalization and the use of acidic anions (e.g. HSO_4^- and $H_2PO_4^-$), which limit the range of viable new compounds that can be developed. In this work, we propose enhancing the intrinsic acidity of imidazolium through functionalization with electron-withdrawing groups, a strategy that resulted in room-temperature Brønsted acidic protic ionic liquids. Specifically, nitro- and cyano-functionalized room temperature protic ionic liquids were successfully synthesised and characterised. Compared to a prototypical protic ionic liquid such as $[C_4HIm][TFSI]$, the addition of a nitro- or cyano-group led to increased acidity, as demonstrated by converging experimental results obtained by spectroscopic methods and molecular modelling. This functionalization significantly impacted thermal and transport properties, with the nitro- and cyano-functionalized protic ionic liquids displaying reduced thermal stability, higher viscosity and lower ionic conductivity. In addition, this functionalization affects the temperature dependence of the ionic conductivity with a supposed influence also on fragility, a parameter that, in the case of ionic liquids, requires more dedicated studies for a more comprehensive understanding.

1. Introduction

From the early days of research in the field of ionic liquids, one of the common arguments in favour of their use as solvent systems has been the possibility of realizing tailor-made ionic liquids by selecting a specific cation-anion combination with properties suited for a particular application; ionic liquids are therefore also known as “designer solvents” [1]. However, this is only true to a certain extent since, although there are ideally numerous combinations of cations and anions, in practice there are limits to their commercial availability or to their synthetic procedures. This limitation is particularly noticeable in less-developed subcategories of ionic liquids, such as acidic ionic liquids and, more specifically, Brønsted acidic ionic liquids.

In brief, acidic ionic liquids possess an acidic moiety, either a Brønsted or a Lewis acidic site, which, in the case of Brønsted acidic ionic liquids, is prone to donate a hydrogen ion (also referred to as H^+, or proton) [2]. Such compounds have been successfully employed in various applications, such as in the transformation of lignocellulosic [3] and marine [4] biomass, in homogeneous [5] and heterogeneous (by the use of support materials [6]) catalysis and as proton conductors in proton exchange membrane fuel cells [7–10]. These compounds offer advantages over traditional organic and inorganic acids, as they can be less corrosive toward metals (some acidic ionic liquids being reported as corrosion inhibitors [11]) or non-corrosive at all [12], can result in higher catalytic activity [2], and can be easier to recycle and are less volatile [13].

The two most common strategies for achieving acidity in ionic liquids involve either the modification of common cation structures (e.g. imidazolium- or alkylammonium-derived cations) with sulfonic acid groups (SO_3H) or the use of acidic anions (e.g. HSO_4^- and $H_2PO_4^-$). These strategies have been thoroughly explored, including increasing the number of acidic moieties in the ionic liquid, for example by anchoring multiple SO_3H groups [14] or by incorporating multi-valent cations with their corresponding multiple acidic anions [15]. These strategies can be used to make Brønsted acidic ionic liquids with a range of different acidities, but the number of ionic liquids achievable and viable using these strategies remains limited. Furthermore, safety concerns arise with the use of sultones, which are used to make SO_3H-functionalized ionic liquids; for instance 1,3-propanesultone is considered a “carcinogenic substance of very high concern” by the Euro-

* Corresponding author.
E-mail address: anna.martinelli@chalmers.se (A. Martinelli).
[1] These authors contributed equally to this work.

https://doi.org/10.1016/j.molliq.2024.126269
Received 27 June 2024; Received in revised form 30 September 2024; Accepted 13 October 2024
Available online 28 October 2024

pean Chemicals Agency [16]. Common protic ionic liquids [17], such as 1-butylimidazolium bis(trifluoromethylsulfonyl)imide ([C_4HIm][TFSI], discussed later in this work), also exhibit a certain degree of acidity due to the cation's N-H group. However, the acidity of typical protic ionic liquids (as determined by the Hammett acidity function) is lower than that of SO_3H-functionalized ionic liquids or a protic ionic liquid providing an acidic anion like HSO_4^- [18].

The focus of this work is to explore the possibility of increasing the acidity of common imidazolium-based protic ionic liquids by modifying the cation with electron-withdrawing groups, such as nitro (NO_2) and cyano (CN) groups. This strategy has been previously explored [19], but it resulted in salts with high melting points (above 120 °C). Our objective was therefore to use this same strategy for increasing the acidity of protic ionic liquids while achieving liquids with a melting point below 25 °C. For this purpose, imidazole-based compounds were first alkylated with longer alkyl chains (i.e. butyl instead of methyl) and the weakly coordinating bis(trifluoromethylsulfonyl)imide (TFSI) was used as the counter-anion (instead of chloride or tosylate). Dicyano functionalization was also explored as an alternative to nitrated compounds, leveraging the commercial availability of 4,5-dicyanoimidazole, commonly synthesized from diaminomaleonitrile. Although these nitro- and cyano-functionalized imidazole compounds have previously been used as azolate anions in aprotic ionic liquids [20,21], as far as we are aware we here provide the first report of room-temperature protic ionic liquids with these functional groups. In addition to presenting details of the synthesis, we also report the fundamental properties of the synthesized protic ionic liquids, investigated through thermal analysis, NMR and FTIR spectroscopy, conductivity measurements and molecular modelling, with an emphasis on rationalizing the correlation between the acidity of the N-H bond and other physicochemical properties.

2. Experimental and theoretical methods

2.1. Materials

4-Nitroimidazole, 4,5-dicyanoimidazole, 1-iodobutane (copper stabilized), anhydrous potassium carbonate, calcium carbonate, activated charcoal (powder, 100 mesh) and 0.6 mL ampules of DMSO-d_6 (99.9% with 0.03% TMS (v/v)) were purchased from Sigma Aldrich, stored in a regular chemical storage cabinet, and used without further purification. The protic ionic liquid 1-butylimidazolium bis(trifluoromethylsulfonyl)imide, [C_4HIm][TFSI], was purchased from Iolitec, stored in the glovebox, and used without further purification. Single-use sachets of an aqueous conductivity standard (12.88 mS/cm) were purchased from Mettler-Toledo, and stored in a regular chemical storage cabinet without any special preparation. Molecular sieves, 3 Å (4–8 mesh), were purchased from Sigma Aldrich, dried in a vacuum oven under full vacuum at 180 °C overnight, and then stored inside a MBRAUN UNIlab Plus Eco glovebox filled with nitrogen gas and equipped with a MB-LMF II solvent absorber system. Trifluoromethanesulforic acid (HTfO, 99.6%, 25 g ampule) and bis(trifluoromethanesulfonyl)amine (HTFSI, 99.5%) were purchased from Sigma Aldrich, stored inside the glovebox and used without further purification. Acetonitrile, acetone, dichloromethane, and 2-methyl tetrahydrofuran, were purchased from various suppliers and used as received. Syringe filters with PTFE membranes (0.22 μm pore size) from FisherBrand were purchased from Fisher Scientific.

2.2. Synthesis of the bases

Both functionalized imidazolium-based compounds, i.e. the bases, were synthesized *via* an amine alkylation reaction using 1-iodobutane, as described further below. Fig. 1 summarizes the reaction conditions used in the synthesis of the nitro- and cyano-functionalized bases.

2.2.1. Synthesis of 1-butyl-4-nitroimidazole

4-Nitroimidazole (10.00 g, 88.44 mmol, 1 eqv.), potassium carbonate (24.4 g, 176.55 mmol, 2 eqv.) and acetonitrile (90 mL) were added

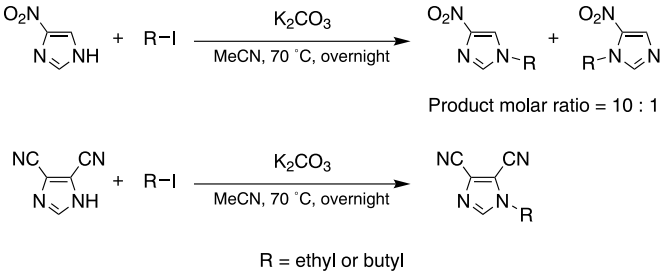

Fig. 1. N-alkylation reactions for the ionic liquids' basic precursors.

to a tree-necked round-bottom flask equipped with a dropping funnel, a condenser with a calcium carbonate drying tube as well as a magnetic stir bar. The mixture was then stirred over an ice bath for a few minutes. 1-Iodobutane (19.52 g, 106.08 mmol, 1.2 eqv.) was added to the dropping funnel and slowly added into the mixture while stirring. Once all of the 1-iodobutane was added, 10 mL of acetonitrile was added to the dropping funnel to wash the remaining 1-iodobutane residue into the reaction mixture. The mixture was then stirred over ice for an additional 10 minutes and subsequently heated to 70 °C overnight. After the end of the reaction, the acetonitrile was removed by rotary evaporation. The crude product was extracted from the evaporation residual material (mainly consisting of inorganic salts) using three increments (40 ml, 30 ml, 30 ml) of 2-methyl-tetrahydrofuran. An orange oil crude product was obtained after the removal of the solvent using rotary evaporation. ^{1}H-NMR was used to determine the composition of this orange oil, which indicated the presence of a substitution isomer (1-butyl-5-nitroimidazole) in a ratio of approximately 1:10 to the main product (1-butyl-4-nitroimidazole). Small-scale Kugelrohr distillation was used to separate these two compounds. At first, the crude mixture was distilled at 160 °C under full vacuum in order to remove any remaining low boiling point compounds. The distillation glassware was then cleaned and the remaining leftover crude product was distilled under full vacuum at 250 °C. The resulting distillate was collected as a liquid, which quickly crystallized into dark orange crystals. This product was further distilled (twice) in the same conditions (full vacuum at 250 °C), resulting in a pale yellow solid. This solid was dissolved in a small volume of acetone, to which activated charcoal was added. This solution was stirred overnight at room temperature. Afterwards, the activated charcoal was removed using a syringe filter, and the acetone evaporated. The resulting off-white crystals were dried (in the Kugelrohr at 60 °C and full vacuum) and transferred into the glovebox. The purity of the final product was estimated, using GC-FID, to be 99.8% (m/m). ^{1}H-NMR (400 MHz, DMSO-d_6, referenced with DMSO-d_6) δ 8.44 (d, 1H), 7.88 (d, 1H), 4.06 (t, J = 7.2 Hz, 2H), 1.74 (m, 2H), 1.21 (m, 2H), 0.87 (t, J = 7.4 Hz, 3H). ^{13}C-NMR (101 MHz, DMSO-d_6, referenced with DMSO-d_6) δ 147.00, 137.39, 121.53, 47.10, 31.97, 18.99, 13.28. The ^{1}H-NMR and ^{13}C-NMR spectra of this base are reproduced in the SI file.

2.2.2. Synthesis of 1-butyl-4,5-dicyanoimidazole

4,5-Dicyanoimidazole (20.00 g, 169.35 mmol, 1 eqv.), potassium carbonate (46.8 g, 338.63 mmol, 2 eqv.) and acetonitrile (190 mL) were added to a tree-necked round-bottom flask equipped with a dropping funnel, a condenser with a calcium carbonate drying tube as well as a magnetic stir bar. The mixture was then stirred over an ice bath for a few minutes. 1-Iodobutane (37.40 g, 203.24 mmol, 1.2 eqv.) was added to the dropping funnel and slowly added into the mixture while stirring. Once all of the 1-iodobutane was added, 10 mL of acetonitrile was added to the dropping funnel to wash the remaining 1-iodobutane residue into the reaction mixture. The mixture was then stirred over ice for an additional 10 minutes and subsequently heated to 70 °C overnight. After the end of the reaction, the acetonitrile was removed by rotary evaporation. The crude product was extracted from the evaporation residual material (mainly consisting of inorganic salts) using three increments (40 ml, 30 ml, 30 ml) of 2-methyl-tetrahydrofuran. A pale yellow oil

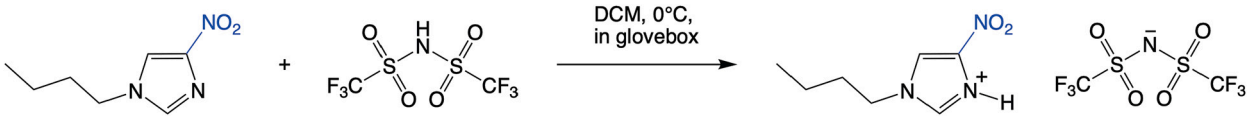

Fig. 2. Neutralization reaction between the base and the acid (left) to obtain the protic ionic liquid [C_4H−4−NO_2Im][TFSI] (right).

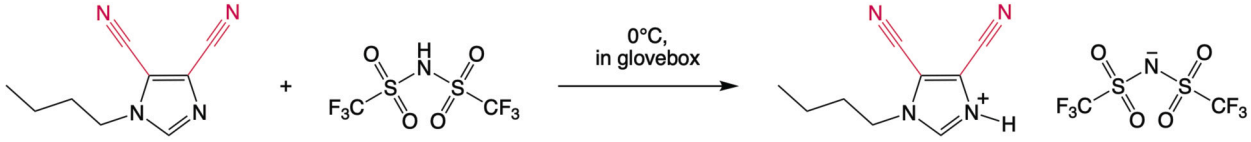

Fig. 3. Neutralization reaction between the base and the acid (left) to obtain the protic ionic liquid [C_4H−4,5−$(CN)_2$Im][TFSI] (right).

crude product was obtained after the removal of the solvent using rotary evaporation. Small-scale Kugelrohr distillation was used to isolate the pure product. The crude oil was distilled in the Kugelrohr at 230 °C under full vacuum, yielding a clear off-white liquid, which was transferred to the glovebox. The purity of the final product was estimated, using GC-FID, to be 99.8%. ^{1}H-NMR (400 MHz, DMSO-d_6, referenced with DMSO-d_6) δ 8.37 (s, 1H), 4.21 (t, J = 7.2 Hz, 2H), 1.78 (m, 2H), 1.27 (m, 2H), 0.90 (t, J = 7.4 Hz, 3H). ^{13}C-NMR (101 MHz, DMSO-d_6, referenced with DMSO-d_6) δ 143.37, 121.21, 112.47, 111.99, 108.66, 47.24, 31.49, 18.94, 13.22. The ^{1}H-NMR and ^{13}C-NMR spectra of this base are reproduced in the SI file.

2.3. Synthesis of the protic ionic liquids

The synthesis of the protic ionic liquids was based on a previously developed method [22]. In brief, the method consists of accurately measuring equimolar amounts of acid and base in a glass syringe and a Schlenk vial and subsequently mixing them over a cooling bath. Most of this procedure is done inside a glovebox, which avoids the issue of moisture absorption by reagents and products. However, the referenced procedure did not allow for cooling inside the glovebox, cooling being necessary during the exothermic neutralization reaction, in order to avoid the decomposition of the protic ionic liquids. In practice, that meant transferring the airtight reaction setup to a nitrogen Schlenk line outside the glovebox and performing the reaction over an ice bath. In the procedure reported here, the cooling was instead performed inside the glovebox using a magnetic stir plate with heating and cooling capabilities (Cambridge Reactor Design - Polar Bear Plus device) and, as a result, the procedure was greatly simplified since the whole reaction setup remained inside the glovebox. Another change with respect to our previously reported method [22] is the use of a solvent for the synthesis of [C_4H−4−NO_2Im][TFSI], since both acid and base are solids, which is incompatible with the original methodology. For more details on the synthesis procedure, please refer to the video in the supporting information of the previously published article [22]. It is finally important to point out that the mass amounts of acid and base used were calculated using a purity correction to achieve equimolar reagent amounts.

2.3.1. Synthesis of [C_4H−4−NO_2Im][TFSI]

HTFSI (19.92 mmol, 1 eqv.) was weighed in a Schlenk vial. 1-Butyl-4-nitroimidazole (19.92 mmol, 1 eqv.) was weighed inside a glass vial, dissolved in dichloromethane (3 ml, dried with molecular sieves) and transferred into a syringe, using another millilitre to extract any residue from the vial, ensuring that the full amount of base was transferred into the syringe. The syringe was then connected to the Schlenk vial (containing the acid and a stir bar) by a PTFE tube, and the setup was placed in a metallic bead cooling bath over the Polar Bear Plus device. The base solution was then slowly added to the acid-containing Schlenk vial, ensuring that the temperature remained low (≈ 0 °C). Once all base was added, the contents of the reaction setup were further mixed by repeatedly filling and emptying the syringe with the reaction mixture. In order to remove the reaction solvent, the Schlenk vial containing the protic ionic liquid solution was capped, removed from the glovebox and attached to a vacuum pump, via a Schlenk line. The solution was stirred and heated at 40 °C overnight. Afterwards, the Schlenk vial containing the clear pale yellow viscous protic ionic liquid was transferred back to the glovebox for storage. No further purification steps were performed. ^{1}H-NMR (800 MHz, neat ionic liquid at 60 °C, referenced with DMSO-d_6 from a capillary tube) δ 12.32 (br, 1H), 8.17 (br, 1H), 7.82 (br, 1H), 3.86 (t, J = 7.8 Hz, 2H), 1.45 (m, 2H), 0.91 (m, 2H), 0.42 (t, J = 7.6 Hz, 3H). ^{13}C-NMR (201 MHz, neat ionic liquid at 60 °C, referenced with DMSO-d_6 from a capillary tube) δ 136.59, 134.36, 120.69, 118.33 (q, J = 320 Hz, CF_3), 50.41, 29.73, 17.48, 10.89. The ^{1}H-NMR and ^{13}C-NMR spectra of this ionic liquid are reproduced in the SI file. The molecular structure of this protic ionic liquid is shown in Fig. 2.

2.3.2. Synthesis of [C_4H−4,5−$(CN)_2$Im][TFSI]

HTFSI (19.37 mmol, 1 eqv.) was weighed in a Schlenk vial. 1-Butyl-4,5-dicyanoimidazole (19.37 mmol, 1 eqv.) was weighed inside the syringe. The syringe was then connected to the Schlenk vial (containing the acid and a stir bar) by a PTFE tube, and the setup was placed in a metallic bead cooling bath over the Polar Bear Plus device. The base was then slowly added to the acid-containing Schlenk vial, ensuring that the temperature remained low (≈ 0 °C). Once all base was added, the contents of the reaction setup were heated to 60 °C (in order to reduce the viscosity of the reaction mixture) and further mixed by repeatedly filling and emptying the syringe with the reaction mixture. Afterwards, the Schlenk vial containing the clear pale yellow viscous protic ionic liquid was capped and stored inside the glovebox. No further purification steps were performed. ^{1}H-NMR (800 MHz, neat ionic liquid at 60 °C, referenced with DMSO-d_6 from a capillary tube) δ 12.37 (br, 1H), 8.34 (br, 1H), 3.88 (br, 2H), 1.47 (br, 2H), 0.93 (br, 2H), 0.47 (br, 3H). ^{13}C-NMR (201 MHz, neat ionic liquid at 60 °C, referenced with DMSO-d_6 from a capillary tube) δ 138.15, 118.23 (q, J = 321 Hz, CF_3), 114.75, 112.00, 103.60, 103.38, 50.47, 29.32, 17.55, 11.00. The ^{1}H-NMR and ^{13}C-NMR spectra of this ionic liquid are reproduced in the SI file. The molecular structure of this protic ionic liquid is shown in Fig. 3.

2.4. NMR spectroscopy

Qualitative NMR data for 1-butyl-4-nitroimidazole and 1-butyl-4,5-dicyanoimidazole were collected using a Varian 400-MR (400 MHz ^{1}H frequency) equipped with a OneNMR probe. Samples were prepared by dissolving a small amount of each base in DMSO-d_6 and loading this solution in a common 5 mm NMR tube. Acquisition of the spectra was performed at 25 °C with spinning at 20 Hz, using standard pulse sequences and acquisition settings for qualitative ^{1}H and ^{13}C available in the VNMRJ 4.2 software. For ^{1}H-NMR, the pulse angle was set to 90°, the relaxation delay was set to 10 s and 16 scans were collected. For ^{13}C-NMR, the relaxation delay was set to 1 s and 256 scans were collected.

A Bruker Avance III HD system with an Oxford 800 MHz (^{1}H frequency) magnet, equipped with a 5 mm TXO cryoprobe, was used to collect the qualitative NMR data for the protic ionic liquids. The pure ionic liquid samples were loaded in common 5 mm NMR tubes fitted with a coaxial capillary tube insert filled with DMSO-d_6. The NMR data was collected at 25 °C and 60 °C without spinning. The standard pulse sequences for qualitative ^{1}H (zg) and carbon ^{13}C (zgzrse) available on the TOPSPIN 3.6.2 software were used. For ^{1}H-NMR, the pulse angle was set to 90°, the relaxation delay was set to 60 s and 4 scans were collected. For ^{13}C-NMR, the relaxation delay was set to 0.1 s and 2048 scans were collected.

Spectral analysis was performed using the MestReNova 14.2.0 software. Apodization (exponential multiplication, 0.3 Hz for ^{1}H NMR and 0.5 Hz and 5 Hz for ^{13}C NMR of bases and ionic liquids respectively), zero filling, automatic phase correction and automatic baseline correction were all performed using default settings. Chemical shifts for ^{1}H and ^{13}C were referenced using the DMSO residual peaks set at 2.50 ppm for ^{1}H and 39.52 ppm ^{13}C.

2.5. Infrared spectroscopy

Infrared spectra were collected at room temperature while the sample was kept under nitrogen gas flow. A Frontier MIR/FIR Spectrometer was used in the ATR (Attenuated Total Reflectance) mode, equipped with a single-point reflection GLADIATR™ diamond crystal from Pike Tech. To minimize moisture absorption during spectral collection, a droplet of the protic ionic liquid (from a syringe wrapped in Parafilm® and prepared inside a glovebox) was carefully placed on the ATR window, while maintaining a flow of dry N_2 gas over it. A total of eight scans were collected within the spectral range of 400 to 4000 cm^{-1}, with a resolution of 2 cm^{-1}. Additionally, a background spectrum was collected and subtracted from the spectra of the protic ionic liquids. For further analysis, all collected spectra were baseline corrected and normalized to the strongest signal. All FTIR spectra in their full spectral range can be found in the supporting information (Fig. S1). When peak fitting was applied to the infrared spectra, a linear baseline and a set of Lorentzian functions were used in the Multipeak Fitting package of the Igor64 software.

2.6. Thermal analysis

2.6.1. Thermogravimetric analysis

Thermogravimetric analysis (TGA) was performed using a Mettler Toledo TGA/DSC 3+ instrument equipped with an autosampler. Sample mass was measured with an XS105 semi-micro balance from Mettler Toledo. Samples were prepared inside the glovebox by loading small amounts of the ionic liquids (around 11–15 mg) inside 70 μL alumina pans without caps. These samples were then transported to the TGA instrument in sealed plastic bags and placed in the autosampler carousel under N_2 flow (by following the sample pan with a N_2 gas hose) and inserted inside the instrument oven as quickly as possible. This was done in order to avoid moisture absorption by the samples before the analysis. Inside the TGA oven, the samples were subjected to a temperature increase from 25 to 500 °C, under a 60 mL/min flow of N_2 and with a heating rate of 8 °C/min. The onset and peak decomposition temperatures (by first derivative analysis) (Table 2), as well as the full thermogravimetric curves (Fig. 6), are presented in the Results and discussion section.

2.6.2. Differential scanning calorimetry

Differential scanning calorimetry (DSC) was performed using a Mettler Toledo DSC 2 instrument equipped with an autosampler. Sample mass was measured with an XS105 semi-micro balance from Mettler Toledo. The samples were prepared inside the glovebox by loading small amounts (around 4–6 mg) of the ionic liquids into 40 μL aluminium pans, which were then hermetically sealed with a sealing press. The crucibles containing the samples were placed in the instrument's autosampler with no special precautions. A heating and cooling rate of 10 °C/min was used to promote glass formation, two cycles were performed in the range from -100 to 60 °C, under a N_2 flow of 100 mL/min. The data obtained from the second cycle is presented in the experimental section (Table 2) and the full thermographs can be found in the supporting information (Fig. S2).

2.7. Ionic conductivity

The ionic conductivity of the protic ionic liquids was measured using the setup described in one of our previous works [23]. In summary, the conductivity of the pure protic ionic liquids (contained in small glass tubes) was measured inside the glovebox using a dip-in type conductivity microprobe and a temperature control system. Data was collected at temperatures ranging from 25 to 80 °C. Due to its higher viscosity, the protic ionic liquid [C_4H−4,5−$(CN)_2$Im][TFSI] was analyzed starting from 80 °C and finishing at 25 °C to reduce viscosity and minimize the risk of trapping bubbles inside the conductivity microprobe. The ionic conductivity setup was calibrated outside the glovebox using single-use sachets of an aqueous conductivity standard of 12.88 mS/cm from Mettler-Toledo. Conductivity values were collected using single samples of the protic ionic liquids.

2.8. Molecular modelling

As a first step in modelling of the single ion pairs of all protic ionic liquids, a search for low-energy conformers was performed using the CREST (v 2.11) software [24]. Default settings were used, with the only modifications being the use of tight optimization settings and acetone implicit solvation using the GBSA model. The top ten lowest energy conformers were selected for the next round of structure refinement, which used the r^{2}SCAN-3c/CPCM(Ethanol) level of theory [25], as implemented in the Orca v5.0.4 software [26]. The settings "TIGTHSCF" and "DEFGRID3" were also employed. The lowest energy conformers for each of the three ionic liquids were submitted to numerical frequency calculations in order to determine the absence of imaginary frequencies, assuring that the final structures were not at a saddle point. Only geometries with no imaginary frequencies were used, if an imaginary frequency was found, these geometries were slightly modified and optimized again until no imaginary frequencies were present. The lowest single-point energy conformers from each ionic liquid were used for a final round of single-point calculations at the ωB97M-V/def2-TZVPD/CPCM(Ethanol) level of theory [27,28], which was used to calculate the conceptual density functional theory (CDFT) descriptors [29,30] (electronegativity and electrophilicity). The xyz files of the final optimized structures of all three ionic liquids (lowest single point energy conformers) can be found in the supporting information.

3. Results and discussion

3.1. Synthetic challenges

While this work reports a method for obtaining butylated nitro- and cyano-functionalized compounds, our initial objective was to make ethylated compounds by performing small-scale ethylation reactions of 4-nitroimidazole and 4,5-dicyanoimidazole. Although 1-ethyl-4,5-dicyanoimidazole could be successfully synthesized, 1-ethyl-4-nitroimidazole proved challenging, specifically in its isolation. This issue can be easily identified by examining at the molecular structure of the two imidazolium precursors and the resulting products (Fig. 1).

Since 4,5-dicyanoimidazole is symmetrical, an electrophilic attack by a single alkyl halide molecule results in a single product, as both ring nitrogens on the imidazole compound are equivalent. However, in the case of 4-nitroimidazole, the asymmetry of the molecule results in two

different substitution products (due to the existence of two different tautomers, 4- and 5-nitroimidazole), 1-ethyl-4-nitroimidazole and 1-ethyl-5-nitroimidazole, with a molar ratio of roughly 10:1 as determined by ^{1}H-NMR. These substitution isomers are extremely similar, and hence difficult to separate due to the marginal differences in physical properties (solubility and boiling point, for instance). Attempts to separate these products by distillation resulted in thermal decomposition due to the high temperatures required. The solution to this problem was to increase the alkyl chain length, from ethyl to butyl, allowing these compounds to be separated at lower temperatures. Multiple rounds of distillation were still required to isolate the major isomer (1-butyl-4-nitroimidazole), resulting in only minute traces of the side product being observed in the ^{1}H-NMR spectrum.

Having synthesized both butylated bases, our next intention was to make four different protic ionic liquids by combining them with HTfO and HTFSI. However, the synthesis of the two TfO-based protic ionic liquids was unsuccessful. During the addition of the acid to the bases, solid products formed (even before the entire amount of acid had been added), which upon heating (up to 80 °C) did not melt. This issue makes the synthesis of these TFO-based compounds incompatible with our setup. Moreover, although these TfO-based compounds could certainly be synthesized with the aid of a solvent, their melting points will likely be way above room temperature, making them less useful for practical applications. Hence, only the TFSI-based compounds were made. The next challenge was to adapt the experimental setup [22] to the use of a solvent, since the precursors for the synthesis of [C_4H−4−NO_2Im][TFSI] are both solids. Dichloromethane was chosen as a solvent for 1-butyl-4-nitroimidazole, since it can be easily removed from the product at low temperatures (avoiding the thermal decomposition of the protic ionic liquid) and it is unreactive towards the HTFSI acid. The primary concern with the use of solvents is that many of them remain in the final product in trace amounts; however, traces of dichloromethane could not be detected in the ^{1}H-NMR nor in the ^{13}C-NMR spectra of [C_4H−4−NO_2Im][TFSI]. To summarize, our synthetic efforts resulted in two new TFSI-based room-temperature protic ionic liquids and two failed attempts to synthesize TfO-based protic ionic liquids; the latter yielding solid compounds that were not further investigated.

3.2. Increased acidity of the N-H bond

NMR spectroscopy was used to confirm the structure of the synthesized protic ionic liquids, but also to examine differences in their N-H bond acidity. The chemical shift of the (N)H hydrogen depends on the proton affinity of the conjugated acid of the anion [31] as well as on the shielding and deshielding effects of the substituting groups on the cation. Given that in our ionic liquid series the anion is in common (TFSI), the experimentally observed changes in the ^{1}H NMR chemical shift can primarily be attributed to the intrinsic structure of the cation. In our case, the addition of the electron-withdrawing groups is expected to pull electrons from the hydrogen (making it more deshielded) and hence cause a downfield shift of the (N)H resonance [32]. The ^{1}H-NMR spectra of the protic ionic liquids studied in this work were collected at two different temperatures, in order to reduce the viscosity and hence produce better resolved spectra (mostly relevant for the case of [C_4H−4,5−$(CN)_2$Im][TFSI]), Fig. 4. To further illustrate the effect of temperature on improving the peak resolution in these spectra, a zoomed-in spectrum for [C_4H−4−NO_2Im][TFSI] can be found in the supporting information (Figure S3).

Upon inspection of the (N)H shifts in the NMR spectral range 11–13 ppm, the effect of the electron-withdrawing groups on the imidazolium cation becomes clear; the unmodified ionic liquid [C_4HIm][TFSI] has the lowest (N)H shift at 11.09 (at 60 °C) whilst the nitro- and cyano-functionalized compounds have peaks at 12.32 and 12.37, respectively. A difference can also be deduced by analyzing the chemical shift of the aromatic hydrogens at the C^2 position (peaks at 7.99, 8.17 and 8.34 ppm), which show the same trend as the (N)H peaks. These trends con-

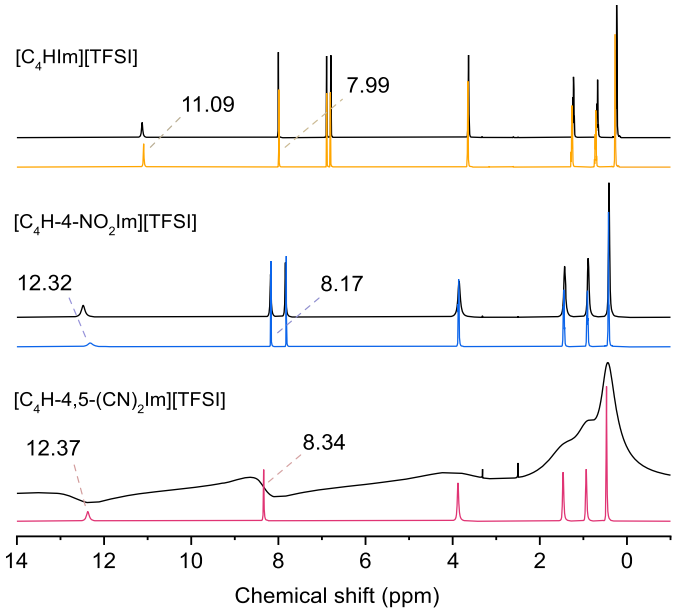

Fig. 4. ^{1}H-NMR spectra of all three protic ionic liquids recorded at two different temperatures, black lines for 25 °C and coloured lines for 60 °C.

firm that the dominating and overall effect of the substituted groups is deshielding, with the electron withdrawing effect through the ring causing the shift and in turn revealing an increased acidity of the N-H bond. A similar effect of increased N-H bond acidity was recently reported upon substitution of imidazolium with triazolium in a series of protic ionic liquids, which was supported by DFT calculations [22].

FTIR spectroscopy was used as a complementary method to investigate the fate of the N-H bonds, Fig. 5. A wide feature peaked at approximately 3260 cm^{-1} and attributed to N-H stretching can be observed in the IR spectrum of [C_4HIm][TFSI], but cannot be as easily observed in the spectra of the other two ionic liquids, Fig. 5a. Since the N-H stretching is expected to be an infrared active mode in all three protic ionic liquids, it is supposedly broadened and red shifted in the case of the functionalised ones. Broadening and red shift was for instance captured when substituting TFSI for TfO in imidazolium based protic ionic liquids, as a consequence of stronger hydrogen bonds between TfO and the -NH group of imidazolium [33]. DFT calculations performed later on for the same systems also predicted such a relative red shift [22].

Since in the IR spectra of the nitro- and cyano-functionalized protic ionic liquids, shown in Fig. 5a, only the high-frequency flank of a broader feature is visible (see also Figure S4 in the SI file), the spectral region 2500 – 3500 cm^{-1} was peak fitted to get deeper insight, as shown in Figures S5–S7 of the SI file. This approach confirms the red shift of the N-H stretching mode moving from the unmodified protic ionic liquid to the cyano-modified one, as visualized in Fig. 5b. The red shift of the N-H stretching mode reflects a longer (weaker) N-H bond and is hence an indication of increased acidity. The relatively strong and well isolated vibrational mode observed in Fig. 5a at ca 3160 cm^{-1} for [C_4HIm][TFSI], clearly red shifts as well in the functionalized ionic liquids; see the trend in Fig. 5b. This mode has a main contribution from C^2-H stretching [22] and, as discussed above for the shifts downfield in the NMR spectra, is also expected to be affected by the presence of the electron-withdrawing groups. For prototypical protic ionic liquids of the family [C_nHIm][TFSI], it is well known that C^2-H is the next most acidic bond in the imidazolium cation following N-H.

3.2.1. Insights from computational molecular modelling

Molecular modelling, in the form of density functional theory (DFT) calculations, can serve as a valuable tool to rationalize the difference in acidity between protic ionic liquids [19,22]. More precisely, the molecular descriptors electronegativity and electrophilicity are used. However,

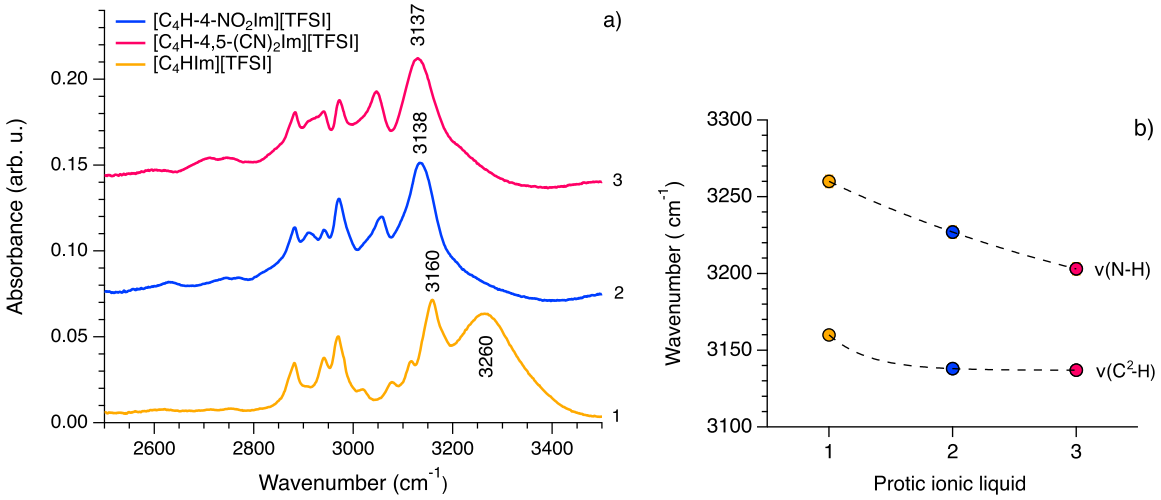

Fig. 5. a) Experimentally recorded FTIR spectra (vertically offset for clarity) of all three ionic liquids, in the frequency region of the N-H and C-H stretching modes. b) Peak positions as found from the peak fit procedure applied to the spectra shown in a).

Table 1
CDFT molecular descriptors for the ion pairs analyzed in the ωB97M-V/def2-TZVPD/CPCM(Ethanol) level of theory.

Protic ionic liquid	Eletronegativity (eV)	Electrophilicity (eV)
$[C_4HIm][TFSI]$	4.7085	2.0504
$[C_4H{-}4{-}NO_2Im][TFSI]$	5.9561	3.6593
$[C_4H{-}4,5{-}(CN)_2Im][TFSI]$	5.6943	3.2998

certain considerations must be discussed before examining the results of these DFT calculations. The first step in any molecular modelling study is the choice of a molecular geometry representative of the system being studied (which in practice means finding low-energy conformers); this study achieved this by using the CREST software to extensively explore the chemical space of these compounds. The use of this software is a clear improvement compared to manually building initial geometries, which can introduce a certain bias towards specific geometries. The software is also capable of testing a fairly large number of geometries (thousands) at a reasonable level of theory (GFNn-xTB) and computational time. Once a few plausible initial geometries are found, these geometries must be refined at a higher level of theory. Commonly, this would be done using fairly computationally expensive DFT functionals, like the popular B3LYP, but more modern functionals, like r^2SCAN-3c [25], can be used to perform excellent geometry optimization calculations at a fraction of the computational cost. The use of such cost-effective functionals allows for the optimization of multiple geometries in a reasonable amount of time. From these final optimized geometries (10 for each ionic liquid), the lowest energy conformer was selected for a final higher level of theory calculation, which was used to calculate CDFT descriptors (Table 1).

Electronegativity relates to the ability of the molecule to attract electrons and electrophilicity can be considered to be a scaling of the electronegativity taking into consideration the hardness of the molecule (hardness being defined as the resistance of the system to changes in the molecular electronic density), which provides information about how susceptible the molecule is to being attacked by a nucleophile. Combined, these descriptors can be used to determine the Lewis acidity of a molecule. The effect of the electron-withdrawing groups is reflected in the values of electronegativity and electrophilicity reported in Table 1. These values reveal $[C_4H{-}4{-}NO_2Im][TFSI]$ to have the highest Lewis acidity, closely followed by $[C_4H{-}4,5{-}(CN)_2Im][TFSI]$, with $[C_4HIm][TFSI]$ having a significantly lower acidity indicator. Even though these descriptors are directly related to Lewis acidity, it is reasonable to assume that the identified trend will be the same in regard to Brønsted acidity [34]. To summarize, $[C_4HIm][TFSI]$ displays a lower acidity than the other two protic ionic liquids, which in turn display quite similar descriptor values.

3.2.2. *Effect of cyano- and nitro-functionalization on thermal and transport properties*

The TGA curves recorded for the two functionalized protic ionic liquids are shown in Fig. 6, while the corresponding thermal data are reproduced in Table 2. Compared to the reference sample $[C_4HIm][TFSI]$, both functionalized protic ionic liquids present a decreased thermal stability, as revealed by their lower decomposition temperature, T_d. In addition, the cyano-functionalized ionic liquid is less stable than the nitro-functionalized one. The thermal decomposition in protic ionic liquids typically starts with a back proton transfer from the cation to the anion, resulting in neutral species that evaporate more easily than ion pairs [35]. Hence, the lower thermal stability of the two protic ionic liquids at focus in this work could be rationalized by the nature of their

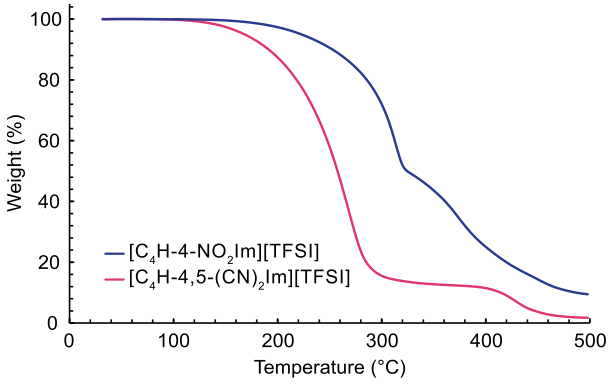

Fig. 6. Thermogravimetric curves recorded for $[C_4H{-}4{-}NO_2Im][TFSI]$ and $[C_4H{-}4,5{-}(CN)_2Im][TFSI]$ in a N_2 atmosphere.

Table 2
Onset and peak decomposition temperatures (estimated from TGA), glass transition temperature (detected by DSC in the 2nd heating scan).

Protic ionic liquid	T_d onset (°C)	T_d peak (°C)	T_g (°C)
$[C_4HIm][TFSI]$[1]	354	N/A	-84
$[C_4H{-}4{-}NO_2Im][TFSI]$	280	314	-41
$[C_4H{-}4,5{-}(CN)_2Im][TFSI]$	218	268	-24

[1] For this ionic liquid, values have been taken from data already published in reference [36].

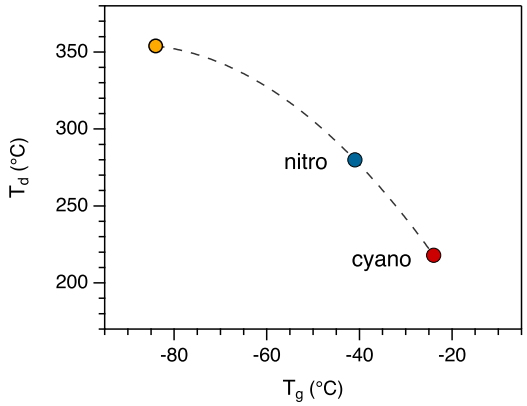

Fig. 7. Onset of the decomposition temperature, T_d, plotted as a function of the glass transition temperature, T_g. The colour code of the symbols is yellow for [C_4HIm][TFSI], blue for [C_4H−4−NO_2Im][TFSI] and red for [C_4H−4,5−$(CN)_2$Im][TFSI].

N-H bond, that under the hypothesis of being more acidic (hence more prone to proton transfer) also become less thermally stable.

The DSC data also show a difference between the thermal properties of these compounds (Table 2). Only glass transitions were detected for the two functionalized protic ionic liquids, similarly to the case of [C_4HIm][TFSI] (for which DSC results have already been published [36]). However, the T_g values of these ionic liquids vary largely, in agreement with the observed and measured viscosity (Table S1), which is lowest for [C_4HIm][TFSI], higher for [C_4H−4−NO_2Im][TFSI] and very high for [C_4H−4,5−$(CN)_2$Im][TFSI]. In other words, the observed viscosities vary accordingly to the recorded T_g values, which in turn follow the inverse trend of T_d. Fig. 7 emphasizes the correlation between higher T_g and lower thermal stability. Higher T_g values typically result from stronger intermolecular interactions.

Importantly, the strength of intermolecular interactions can also affect the macroscopically measured ionic conductivity, shown in Fig. 8 for the three protic ionic liquids at focus in this study. In the representation of an Arrhenius plot, Fig. 8a, the ionic conductivity is clearly the highest for [C_4HIm][TFSI], followed by [C_4H−4−NO_2Im][TFSI] and then by [C_4H−4,5−$(CN)_2$Im][TFSI], a sequence that follows the trend of the measured T_g values (that is, the higher the glass transition temperature, the lower the ionic conductivity at a defined absolute temperature). This, along with the fact that the data points follow a curved rather than a linear behaviour, suggests that the vehicular mechanism dominates in the transport of molecular charges, as previously concluded for many other ionic liquid systems [23,36,37].

In the representation of a T_g-scaled plot as shown in Fig. 8b, however, the trend is reversed, with the values for the nitro- and cyano-modified ionic liquids falling on a common curve, above that of [C_4HIm][TFSI]. This can be the result of a higher fragility of these two ionic liquids, whose ionic conductivity changes more rapidly upon heating from T_g (i.e. departing from $T_g/T = 1$). Based on the current knowledge about fragility in ionic liquids [37], in fragile ionic liquids transport properties like the ionic conductivity change rapidly upon heating from T_g (or vice versa, upon cooling towards T_g), while strong liquids display a closer to linear behaviour, in a T_g-scaled Arrhenius plot. The cause of fragility in protic ionic liquids is not yet well understood, but these results indicate that cation acidity may have an influence. One could also invoke the smaller ΔpKa value as a prediction for higher fragility, as previously proposed in the literature [38] and discussed while comparing triazolium- with imidazolium-based protic ionic liquids [23]. However, to gain deeper insights into this matter more dedicated and systematic studies would be needed, including a larger variation of ionic liquid types.

3.3. Conclusions

In this work, we report a synthetic route to synthesize highly pure imidazolium based protic ionic liquids, functionalized with cyano or nitro groups. In practice, nitro- and cyano-functionalized imidazole bases were first synthesized and isolated in high purity, then successfully used to obtain two new TFSI-based room-temperature protic ionic liquids. Their properties are characterized and compared to those of a prototypical protic ionic liquid, i.e. [C_4HIm][TFSI].

Taken altogether, the shift downfield of the (N)H proton and of the (C^2)H proton in the ^{1}H-NMR spectra, the red shift of both the N-H and the C^2-H stretching modes in the FTIR spectra, and the higher electrophilicity/electronegativity values determined by molecular modelling confirm the hypothesis that anchoring an electron-withdrawing group to the imidazolium cation increases the acidity of the N-H bond. Such an effect is known to result in stronger intermolecular interactions through hydrogen bonding. The experimental observations of lower thermal stability, higher glass transition temperature and hence lower ionic conductivity, synergetically converge in supporting the conclusion above of an increased acidity by cyano- or nitro- functionalization. Interestingly, despite the lower ionic conductivity on a scale of absolute

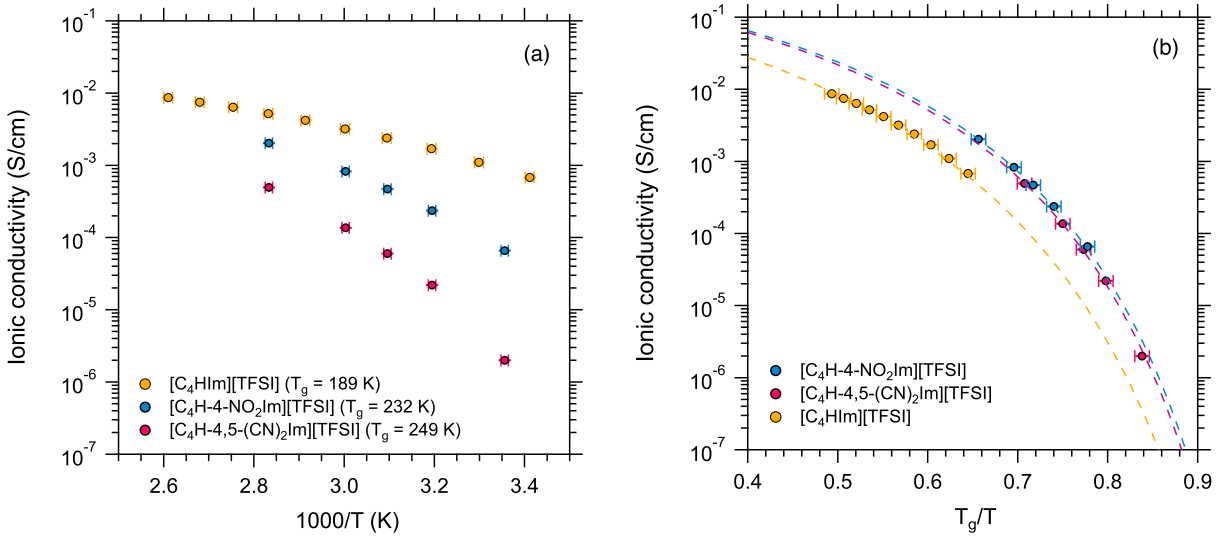

Fig. 8. Arrhenius plot of the ionic conductivity displayed by the three glass-forming protic ionic liquids. (b) T_g-scaled plot (aka Angell plot) with the same experimental data shown in (a). Dashed lines are fits to the experimental data. For [C_4HIm][TFSI], original data from a previous study are reproduced [36].

temperatures, these functionalized protic ionic liquids appear to have a higher fragility, a property that may correlate to acidity/intermolecular interactions but certainly needs further attention and investigation.

A potential application for these Brønsted acidic ionic liquids is in catalysis, where they could substitute other, more conventional ionic liquids. Their high viscosity and low conductivity makes them poor electrolytes for the conduction of ions, however, whether the higher acidity also impacts the local exchange mechanisms of protons remains unexplored, and may be an aspect to be studied in the future. In a broader perspective, the proposed strategy to achieve higher acidity may be used to modify other cations than the imidazolium, addressing applications beyond electrochemistry. Finally, based on the experience through this work, we also believe that it will be a challenge to find weakly coordinating anions alternative to TFSI that still result in liquid compounds at room temperature when reacted with nitro- or cyano-functionalized imidazolium.

CRediT authorship contribution statement

Eva Dahlqvist: Writing – review & editing, Writing – original draft, Visualization, Validation, Methodology, Investigation, Formal analysis, Data curation. **Eduardo Maurina Morais:** Writing – review & editing, Writing – original draft, Visualization, Validation, Methodology, Investigation, Formal analysis, Data curation, Conceptualization. **Anna Martinelli:** Writing – review & editing, Validation, Supervision, Project administration, Funding acquisition.

Declaration of competing interest

The authors declare that they have no known competing financial interests or personal relationships that could have appeared to influence the work reported in this paper.

Acknowledgement

The authors acknowledge funding from the Knut and Alice Wallenberg Foundation (Wallenberg Academy Fellows, grant 2016–0220), the Swedish Research Council (project grant 2018, grant no 05207) as well as the Chalmers Area of Advance Materials Science for supporting an Amanuensis position. The authors would also like to acknowledge the Competence Centre Tech4H2. Tech4H2 is hosted by Chalmers University of Technology and is financially supported by the Swedish Energy Agency (P2021-90268) and the member companies Volvo, Scania, Siemens Energy, GKN Aerospace, PowerCell, Oxeon, RISE, Stena Rederier AB, Johnsson Matthey and Insplorion. The authors also thank the Swedish NMR Centre in Gothenburg for the allocated spectrometer time and Ratchawit Janewithayapun for his help with the viscosity measurements.

Appendix A. Supplementary material

Supplementary material related to this article can be found online at https://doi.org/10.1016/j.molliq.2024.126269.

The Supplementary file contains additional FTIR as well as ^{1}H and ^{13}C-NMR spectra, viscosity data and method description, full DSC thermographs, details of the peak fit procedure, and xyz files of the optimized ionic liquids' structures.

Data availability

Data will be made available on request.

References

[1] SOLVENTS DESIGNER, Chem. Eng. News Arch. 76 (1998) 32–37.
[2] A.S. Amarasekara, Acidic ionic liquids, Chem. Rev. 116 (2016) 6133–6183.
[3] A.M. Asim, M. Uroos, S. Naz, M. Sultan, G. Griffin, N. Muhammad, A.S. Khan, Acidic ionic liquids: promising and cost-effective solvents for processing of lignocellulosic biomass, J. Mol. Liq. 287 (2019) 110943.
[4] L. Liu, Production of chemicals from marine biomass catalysed by acidic ionic liquids, Green Chem. 23 (2021) 9800–9814.
[5] M. Vafaeezadeh, H. Alinezhad, Brønsted acidic ionic liquids: green catalysts for essential organic reactions, J. Mol. Liq. 218 (2016) 95–105.
[6] A. Wolny, A. Chrobok, Silica-based supported ionic liquid-like phases as heterogeneous catalysts, Molecules 27 (2022).
[7] H. Hou, H.M. Schütz, J. Giffin, K. Wippermann, X. Gao, A. Mariani, S. Passerini, C. Korte, Acidic ionic liquids enabling intermediate temperature operation fuel cells, ACS Appl. Mater. Interfaces 13 (2021) 8370–8382.
[8] K. Wippermann, C. Korte, Effects of protic ionic liquids on the oxygen reduction reaction – a key issue in the development of intermediate-temperature polymer-electrolyte fuel cells, Curr. Opin. Electrochem. 32 (2022) 100894.
[9] K. Wippermann, Y. Suo, C. Korte, Oxygen reduction reaction kinetics on pt in mixtures of proton-conducting ionic liquids and water: the influence of cation acidity, J. Phys. Chem. C 125 (2021) 4423–4435.
[10] Z. Wojnarowska, A. Lange, A. Taubert, M. Paluch, Ion and proton transport in aqueous/nonaqueous acidic ionic liquids for fuel-cell applications–insight from high-pressure dielectric studies, ACS Appl. Mater. Interfaces 13 (2021) 30614–30624.
[11] S. Cao, D. Liu, H. Ding, J. Wang, H. Lu, J. Gui, Task-specific ionic liquids as corrosion inhibitors on carbon steel in 0.5 M HCl solution: an experimental and theoretical study, Corros. Sci. 153 (2019) 301–313.
[12] D.-J. Tao, X.-M. Lu, J.-F. Lu, K. Huang, Z. Zhou, Y.-T. Wu, Noncorrosive ionic liquids composed of [HSO4] as esterification catalysts, in: Special Section: Symposium on Post-Combustion Carbon Dioxide Capture, Chem. Eng. J. 171 (2011) 1333–1339.
[13] P. Wasserscheid, Volatile times for ionic liquids, Nature 439 (2006) 797.
[14] D.-Q. Xu, J. Wu, S.-P. Luo, J.-X. Zhang, J.-Y. Wu, X.-H. Du, Z.-Y. Xu, Fischer indole synthesis catalyzed by novel SO3H-functionalized ionic liquids in water, Green Chem. 11 (2009) 1239–1246.
[15] A. Brzęczek-Szafran, J. Więcławik, N. Barteczko, A. Szelwicka, E. Byrne, A. Kolanowska, M. Swadźba Kwaśny, A. Chrobok, Protic ionic liquids from di- or triamines: even cheaper Brønsted acidic catalysts, Green Chem. 23 (2021) 4421–4429.
[16] https://echa.europa.eu/substance-information/-/substanceinfo/100.013.017.
[17] T.L. Greaves, C.J. Drummond, Protic ionic liquids: properties and applications, Chem. Rev. 108 (2008) 206–237.
[18] P. Lu, Z.-P. Zhao, X.-Y. Wang, G.-J. Lan, X.-L. Wang, Understanding effect of molecular structure of imidazole-based ionic liquids on catalytic performance for biomass inulin hydrolysis, Mol. Catal. 435 (2017) 24–32.
[19] E.M. Morais, I.B. Grillo, H.K. Stassen, M. Seferin, J.D. Scholten, The effect of an electron-withdrawing group in the imidazolium cation: the case of nitro-functionalized imidazolium salts as acidic catalysts for the acetylation of glycerol, New J. Chem. 42 (2018) 10774–10783.
[20] A.R. Katritzky, S. Singh, K. Kirichenko, M. Smiglak, J.D. Holbrey, W.M. Reichert, S.K. Spear, R.D. Rogers, In search of ionic liquids incorporating azolate anions, Chemistry 12 (2006) 4630–4641.
[21] M. Smiglak, C. Hines, T. Wilson, S. Singh, A. Vincek, K. Kirichenko, A. Katritzky, R. Rogers, Ionic liquids based on azolate anions, Chemistry 16 (2010) 1572–1584.
[22] E.M. Morais, I. Abdurrokhman, A. Martinelli, Solvent-free synthesis of protic ionic liquids. Synthesis, characterization and computational studies of triazolium based ionic liquids, J. Mol. Liq. 360 (2022) 119358.
[23] E.M. Morais, A. Idström, L. Evenäs, A. Martinelli, Transport properties of protic ionic liquids based on triazolium and imidazolium: development of an air-free conductivity setup, Molecules 28 (2023).
[24] P. Pracht, F. Bohle, S. Grimme, Automated exploration of the low-energy chemical space with fast quantum chemical methods, Phys. Chem. Chem. Phys. 22 (2020) 7169–7192.
[25] S. Grimme, A. Hansen, S. Ehlert, J.-M. Mewes, r2SCAN-3c: a "Swiss army knife" composite electronic-structure method, J. Chem. Phys. 154 (2021) 064103.
[26] F. Neese, F. Wennmohs, U. Becker, C. Riplinger, The ORCA quantum chemistry program package, J. Chem. Phys. 152 (2020) 224108.
[27] N. Mardirossian, M. Head-Gordon, ωB97M-V: a combinatorially optimized, range-separated hybrid, meta-GGA density functional with VV10 nonlocal correlation, J. Chem. Phys. 144 (2016) 214110.
[28] D. Rappoport, F. Furche, Property-optimized Gaussian basis sets for molecular response calculations, J. Chem. Phys. 133 (2010) 134105.
[29] P. Geerlings, F. De Proft, W. Langenaeker, Conceptual density functional theory, Chem. Rev. 103 (2003) 1793–1874.
[30] P.K. Chattaraj, D.R. Roy, Update 1 of: electrophilicity index, Chem. Rev. 107 (2007) PR46–PR74.
[31] S.K. Davidowski, F. Thompson, W. Huang, M. Hasani, S.A. Amin, C.A. Angell, J.L. Yarger, NMR characterization of ionicity and transport properties for a series of diethylmethylamine based protic ionic liquids, J. Phys. Chem. B 120 (2016) 4279–4285.
[32] A.-u. Rahman, Nuclear Magnetic Resonance. Basic Principles, Springer US, 1986.
[33] M. Yaghini, J. Pitawala, A. Matic, A. Martinelli, Effect of water on the local structure and phase behavior of imidazolium-based protic ionic liquids, J. Phys. Chem. B 19 (2015).
[34] K. Gupta, D. Roy, V. Subramanian, P. Chattaraj, Are strong Brønsted acids necessarily strong Lewis acids?, J. Mol. Struct., Theochem 812 (2007) 13–24.

[35] M.S. Miran, H. Kinoshita, T. Yasuda, M.A.B.H. Susan, M. Watanabe, Physicochemical properties determined by ΔpKa for protic ionic liquids based on an organic super-strong base with various Brønsted acids, Phys. Chem. Chem. Phys. 14 (2012) 5178–5186.

[36] I. Abdurrokhman, K. Elamin, O. Danyliv, M. Hasani, J. Swenson, A. Martinelli, Protic ionic liquids based on the alkyl-imidazolium cation: effect of the alkyl chain length on structure and dynamics, J. Phys. Chem. B 123 (2019) 4044–4054.

[37] P. Sippel, P. Lunkenheimer, S. Krohns, E. Thoms, A. Loidl, Importance of liquid fragility for energy applications of ionic liquids, Sci. Rep. 5 (2015) 13922.

[38] K. Ueno, Z. Zhao, M. Watanabe, C.A. Angell, Protic ionic liquids based on decahydroisoquinoline: lost superfragility and ionicity-fragility correlation, J. Phys. Chem. B 116 (2012) 63–70.